Published in final edited form as:
Cancer Res. 2013 July 15; 73(14): 4349–4361. doi:10.1158/0008-5472.CAN-13-0322.

Peroxisome proliferator-activated receptor δ (PPARδ) induces estrogen receptor-positive mammary neoplasia through an inflammatory and metabolic phenotype linked to mTor activation

Hongyan Yuan[1], **Jin Lu**[1], **Junfeng Xiao**[1], **Geeta Upadhyay**[1], **Rachel Umans**[5], **Bhaskar Kallakury**[2], **Yuhzi Yin**[3], **Michael E. Fant**[4], **Levy Kopelovich**[6], and **Robert I. Glazer**[1]

[1]Department of Oncology and Lombardi Comprehensive Cancer Center, Lombardi Comprehensive Cancer Center, Georgetown University, Washington, DC 20007

[2]Department of Pathology, Georgetown University, Washington, DC 20007

[3]Laboratory of Allergic Diseases, National Institute of Allergy and Infectious Diseases, Bethesda, MD 20814

[4]Department of Pediatrics, University of South Florida, Tampa, FL 33606

[5]University of Chicago, Chicago, IL

[6]Chemoprevention Agent Development and Research Group, Division of Cancer Prevention, National Cancer Institute, Bethesda, MD 20814

Abstract

The peroxisome proliferator-activated receptor-δ (PPARδ) regulates a multitude of physiological processes associated with glucose and lipid metabolism, inflammation and proliferation. One or more of these processes are potential risk factors for the ability of PPARδ agonists to promote tumorigenesis in the mammary gland. In the present study, we describe a new transgenic mouse model in which activation of PPARδ in the mammary epithelium by endogenous or synthetic ligands resulted in progressive histopathological changes that culminated in the appearance of estrogen receptor- and progesterone receptor-positive and ErbB2-negative infiltrating ductal carcinomas. Multiparous mice presented with mammary carcinomas after a latency of 12 months, and administration of the PPARδ ligand GW501516 reduced tumor latency to five months. Histopathological changes occurred concurrently with an increase in an inflammatory, invasive, metabolic and proliferative gene signature, including expression of the trophoblast gene, Plac1, beginning one week after GW501516 treatment, and remained elevated throughout tumorigenesis. The appearance of malignant changes correlated with a pronounced increase in phosphatidylcholine and lysophosphatidic acid metabolites, which coincided with activation of Akt and mTor signaling that were attenuated by treatment with the mTor inhibitor everolimus. Our

Corresponding Author: Robert I. Glazer, Georgetown University, 3970 Reservoir Rd, NW, Washington, DC 20007. glazerr@georgetown.edu.

Note: Supplementary data for this article are available at Cancer Research Online (http://cancerres.aacrjournals.org)

Disclosure of Potential Conflicts of Interest
No potential conflicts of interest were disclosed by the other authors.

AUTHOR CONTRIBUTIONS
R.I.G. AND L.K. conceived of the hypothesis. R.I.G., H.Y., J.X., G.U. and Y.Y. designed the experiments. H.Y., J.X., J.L., J.X., G.U., R.U. and Y.Y. performed the experiments. R.I.G., H.Y., J.L., J.X. G.U. and Y.Y. analyzed and interpreted the data. M.E.F. provided the Plac1 antibody. R.I.G., H.Y. and L.K. wrote the manuscript.

COMPETING FINANCIAL INTERESTS
The authors declare no financial interests.

findings are the first to demonstrate a direct role of PPARδ in the pathogenesis of mammary tumorigenesis, and suggest a rationale for therapeutic approaches to prevent and treat this disease.

Keywords

PPARδ; transgenic; tumorigenesis; mTor; Plac1

Introduction

The peroxisome proliferator-activated receptors (PPARs) represent a subfamily of ligand-dependent nuclear receptors that regulate the transcription of a multitude of processes associated with metabolism, angiogenesis, inflammation and proliferation (1, 2). Of the three isotypes, PPARδ/β alone was shown more than a decade ago to stimulate mitotic clonal expansion of progenitor cells (3, 4). It was conceivable, therefore, that the selective PPARδ agonist GW501516 (GW) (5) would act as a tumor promoter in mammary carcinogenesis, which proved to be the case (6) (reviewed in (7, 8)). GW and related agonists enhance adenoma size and angiogenesis in APC^{min} mice (9, 10) and stimulate the growth of several lung (11), breast and prostate cancer cell lines (12, 13), although results to the contrary have also been reported (14). Conversely, disruption of PPARδ expression in colon cancer cells by somatic cell knockout (15) or RNA aptamers (16) inhibited tumor cell growth. These findings are consistent with those demonstrating that homozygous deletion of PPARδ reduces tumorigenesis in MMTV-Cox2 mice (17), intestinal adenomas in APC^{min} mice (18), colon carcinogenesis (19) and pancreatic tumor xenograft growth and angiogenesis in stromal tissue (20). Clinically, PPARδ is an important prognostic marker, wherein 50% of invasive breast cancers expressed moderate to high levels of PPARδ protein (7), and 65% of invasive breast cancer expressed elevated levels of PPARδ mRNA, whereas, the reverse is true for normal breast (www.oncomine.org; TCGA database). That high expression of PPARδ mRNA was associated with poor survival in breast cancer patients regardless of subtype (21), emphasizes the importance of this nuclear receptor in this disease.

Obesity and inflammation are cancer risk factors (22) that ultimately result in the generation of endogenous PPARδ ligands (23). These include arachidonic acid metabolites prostaglandin PGI_2 (24) synthesized via Cox2/Pges2 (25), 15-HETE (26) and polyunsaturated fatty acids (27–29). GW increased arachidonic and linoleic acid levels in the mammary gland during carcinogenesis (30), which was associated with activation of PDK1 and Akt (30–32) and reduction of PTEN (11, 33), signaling pathways that facilitate mammary hyperplasia (30, 34, 35). Although, the aforementioned studies implicate PPARδ as a modulator of tumorigenesis, there is no conclusive evidence that PPARδ *per se* is oncogenic. In the present study, we demonstrate that activation of PPARδ in the mammary gland functions as an unconventional oncogene by inducing tumorigenesis, an invasive, metabolic and proliferative and inflammatory gene expression signature, a pronounced increase in phospholipid, lysophosphatidic acid (LPA) and phosphatidic acid (PA) biosynthesis, and mTor pathway activation. These results demonstrate that PPARδ functions as an initiator of mammary tumorigenesis, and suggest new therapeutic options for the prevention and treatment of this disease.

Materials and Methods

Materials

GW501516 was synthesized as previously described (36), and was provided by the Chemoprevention Branch, National Cancer Institute, NIH, Bethesda, MD.

Animals

MMTV-PPARδ mice were generated by pronuclear injection of FVB mouse embryos as previously described (37). The mouse PPARδ cDNA (38) was provided by Dr. Paul Grimaldi, INSERM, Faculté de Médecine, Nice, France, and amplified and cloned into the *Eco*R1 site in MMTV-SV40-Bssk provided by Dr. William Muller, McMaster University, Hamilton, Ontario, Canada. All inserts were confirmed by sequencing. The MMTV- PPARδ construct was digested with *Sal* I-*Spe* I, purified and used for microinjection. Positive animals were identified by PCR using three primer pairs: 1) PPARd-forward: TCT TCA TCG CGG CCA TCA TT, and SV40PolyA-reverse: GTC CAA TTA TGT CAC ACC ACA GAA G, which amplifies a 245 bp transgene fragment, 2) PPARd-forward: GCA TGA AGC TCG AGT ATG AGA AGT G, PPARd-reverse: CTT AGA GAA GGC CTT CAG GTC, which amplifies a 1.2 kbp genomic fragment and a 245 bp cDNA fragment, and 3) PPARd-forward: CCT TTG TCA TCC ACG ACA TC and MMTV-reverse: TCA GCA GTA GCC TCA TCA TC, which amplifies a 870 bp transgene fragment.

Animals were fed either Purina 5001 Rodent Chow or chow supplemented with 0.005% (w/w) GW (6). Everolimus (provided by Novartis) was administered at doses of 10 and 20 mg/kg/d as a nanoemulsion diluted in water by oral gavage for 14 days beginning four weeks after mice were placed on the GW diet. All animal studies were conducted under protocols approved by the Georgetown University Animal Care and Use Committee in accordance with NIH guidelines for the ethical treatment of animals.

Statistical analysis

Statistical analyses were conducted using a two-sided log rank test using GraphPad Prism version 4.03. Differences were consider significant at $P<0.05$.

Histopathology, immunohistochemistry (IHC) and western blotting

Mammary tissue and tumors were excised, and formalin-fixed, paraffin-embedded sections were prepared for H&E staining and IHC. Antigen retrieval was carried out by incubation of tissue sections in 10 mM sodium citrate buffer (pH 6.0) for 20 min at a sub-boiling temperature in an electric steamer as previously described (6, 37). Endogenous peroxidase activity was quenched with 3% hydrogen peroxide for 10 min, and incubated for 30 min with blocking solution (10% goat serum in Tris-buffered saline), followed by incubation overnight at 4°C with the appropriate primary antibody diluted in blocking solution. Biotin-conjugated secondary antibodies were diluted in TBS containing 0.1% Tween-20 and incubated for 30 min at room temperature using the ABC Vectastain (Vector Laboratories) detection system and diaminobenzidine (Pierce), and slides were counterstained with Harris-modified hematoxylin (Thermo-Fisher, Inc.), dehydrated and mounted in Permount (Thermo-Fisher, Inc.). Western blotting was carried out as previously described (6, 30, 37, 39, 40). Antibodies and their dilutions for IHC and western blotting are listed in Supplementary Table 1.

Gene microarray analysis

Microarray analysis was carried out as previously described (6, 30, 37, 39, 40). Briefly, tissue was excised, washed in phosphate-buffered saline and stored in RNAlater (Ambion) at −20°C until RNA extraction. Tissue was snap-frozen in liquid nitrogen, pulverized in a mortar and pestle and RNA extracted using an RNeasy Mini Kit (Qiagen) according to the manufacturer's protocol. RNA purity was assessed by an A_{260}/A_{280} ratio of >1.9, and by the integrity of 18S and 28S rRNA using an Agilent microfluidic chip. Array analysis was carried out on cRNA prepared from equal amounts of RNA (1 μg) pooled from 5 mice per group. Biotin-labeled cRNA was fragmented at 94°C for 35 min and hybridized overnight to

an Affymetrix mouse 430A 2.0 GeneChip® representing approximately 14,000 annotated mouse genes. GeneChip®'s were scanned with an Agilent Gene Array scanner, and grid alignment and raw data generation with the Affymetrix GeneChip® Operating software 1.1. A noise value (*Q*) based on the variance of low-intensity probe cells was used to calculate a minimum threshold for each GeneChip. Samples were averaged and data refined by eliminating genes with signal intensities <300 in both comparison groups, and heat maps were generated from ≥3-fold changes in gene expression normalized to control tissue using unsupervised hierarchical cluster analysis as previously described (41). Gene interaction and ontology analysis utilized Ariadne Pathway Studio version 9.1 (Supplementary Fig. 3). Data sets have been deposited in the GEO public database under accession no. GSE34109.

Quantitative real-time polymerase chain reaction (qRT-PCR)

Total RNA was extracted as described above, and equal amounts of RNA (1 μg) were pooled from each group (five samples per group) and reverse transcribed with the Omniscript RT kit (Qiagen) in a total volume of 20 μl as previously described (6, 30, 37, 39, 40). PCR was performed in triplicate using an ABI-Prism 7700 (Applied Biosystems, Foster City, CA) with SYBRGreen I detection (Qiagen) according to the manufacturer's protocol. Amplification using the appropriate primers (Supplementary Table 2) was confirmed by ethidium bromide staining of the PCR products on an agarose gel. The expression of each target gene was normalized to GAPDH and is presented as the ratio of the target gene to GADPH expression calculated using the formula, $2^{-\Delta Ct}$, where $\Delta Ct = Ct^{Target} - Ct^{18s}$ (39).

Metabolomic analysis

Analysis was performed using ultraperformance liquid chromatography electrospray ionization time-of-flight mass spectrometry (UPLC-ESI-TOFMS)(42) by the Proteomic and Metabolomic Shared Resource, Lombardi Comprehensive Cancer Center, Georgetown University. Experimental groups consisted of mammary glands from each of five control wild-type and transgenic littermates and an equal number maintained on a diet containing 0.005% GW for 11 weeks (6, 30). Tissue was snap-frozen in liquid nitrogen and stored at −80°C. Extracts were prepared in 1 ml chilled 50% methanol containing internal standards (debrisoquine, 1 ng/ml and nitrobenzoic acid, 5 ng/ml) using MagNAlyser Green Beads and a MagNA Lyser agitator (Roche). Samples were clarified, and processing and multivariate analysis performed as described (42). Each sample (5 μl) was injected onto a reverse-phase 50 × 2.1 mm ACQUITY® 1.7-μm C18 column (Waters Corp, Milford, MA) using an ACQUITY® UPLC system (Waters) with a gradient mobile phase consisting of water containing 0.1% formic acid (A), acetonitrile containing 0.1% formic acid (B) and 90% isopropyl alcohol in acetonitrile containing 0.1% formic acid and 10 mM ammonium formate (C) at a flow rate was 0.5 ml/min. The gradient consisted of 98% A for 1.0 min then a ramp to 60% B from 1.0 to 4.0 min, then a ramp to 100% B from 4.0 to 7.0 min, followed by a ramp to 80% C from 7.0 to 9.0 min, and a ramp to 98% A from 9.0–12.0 min. The column eluent was introduced directly into the mass spectrometer by electrospray. Mass spectrometry was performed on a G2 QTOF (Waters) operating in both negative and positive ionization mode with a capillary voltage of 3,000 V in positive mode and 2,500 V in negative mode with a sampling cone voltage of 40 V in both modes. The desolvation gas flow was set to 750 liters/h and the temperature was set to 350 °C. The cone gas flow was 25 liters/hr, and the source temperature was 120°C. Accurate mass was maintained by introduction of the lock mass of leucine-enkephalin under a flow rate of 2 μl/min for the positive mode (556.277 $[M+H]^+$ and 3 μl/min for the negative mode (554.261 $[M+H]^-$) at a concentration of 250 ng/μl in 50% aqueous acetonitrile using LockSpray® interface. UPLC-QTOF data were acquired in centroid mode under full scanning from 50 to 1200 *m/z* (mass-to-charge ratio) using MassLynx software (Waters).

UPLC-QTOF datasets and analysis—Each sample was run in duplicate in both positive and negative modes and the raw data was converted into Network Common Data Form (NetCDF) using MassLynx software. The XCMS package (43) was used to preprocess each of three UPLC-QTOF MS datasets separately. To enable further analysis and visualization of the datasets, all m/z values were binned to fixed m/z values with a bin size of 100 ppm. As a result, the data were transformed into a two dimensional matrix of ion abundances. Rows of the matrix represent the ions with specific retention time (RT) and (m/z) values, while columns represent the individual samples. After detecting ions in individual samples, they were aligned across all samples within the corresponding experiment to allow calculation of RT deviations and relative ion intensity comparison. The parameter design for XCMS package was optimized for UPLC/Q-TOF high resolution LC/MS data according to (44). The ions with Fold change>1.5, $p<0.01$ were selected for further analysis. Total ion Chromatograms plot, Mirror plot, PCA analysis result were provided by XCMS online, box plot and EIC peaks were also generated and sorted in the order of most significant to the least. To select ions with significant and consistent changes between case and controls, the meta analysis was designed to determine overlapping ions among multiple experiments by taking into consideration the presence of a large number of derivative ions such as isotopes, adducts and fragments. Specifically, the approach used groups ions on the basis of ion annotation obtained using R-package CAMERA. Each ion in a cluster is represented by its monoisotopic mass. This mass is then used to compare ions across multiple experiments. The resulting ion list provides better coverage and more accurate identification of metabolites then those obtained by the traditional approach in which overlapping ions are selected on the basis of their ion mass and merged with those obtained on the basis of their monisotopic mass calculated through ion annotation. Putative identifications for the resulting ion list were obtained through a mass-based search against two databases: Metlin, and Madison Metabolomics Consortium Database (MMCD). The mass tolerance in the database search was set to 10 ppm for both positive and negative mode data. The m/z values of annotated isotopes/adducts/neutral-loss fragments peaks were converted to the corresponding neutral monoisotopic masses before searching them against the databases. Identities of some putative metabolite identifications were verified by comparing their MS/MS fragmentation patterns and RT with those of authentic standard compounds.

RESULTS

PPARδ transgene activation induces mammary tumorigenesis

Transgenic mice were generated that expressed the murine PPARδ cDNA under the control of the MMTV 3′-LTR (45) as previously described (30, 35, 37). Two founder lines with germline transmission were identified and founder M-23 was used for further studies (Supplementary Fig. 1A-D). Transgenic animals exhibited increased ductal branching beginning at 6 weeks of age, which markedly increased after animals were administered a diet supplemented with the PPARδ agonist GW (46) for as little as one week (Supplementary Fig. 1E). Maintenance on the GW diet for 6–11 weeks resulted in the appearance of abnormal nodules (Supplementary Fig. 1E) that were positive for Ki-67 (Supplementary Fig. 1F). Multiparous female transgenic mice at 12 months of age presented with multifocal moderate to well-differentiated infiltrating ductal carcinomas, and tumor latency was reduced to five months after administration of the GW diet (Fig. 1A,B). To obtain a sense of the stochastic changes associated with tumorigenesis, transgenic and wild-type mice were fed the GW diet for varying intervals (Fig. 1C). Administration of the GW diet for one to six week resulted in a progressive increase in ductal dilitation with inspissated protein and lipid secretions and areas of atypical ductal and lobular dysplasia. By 11 weeks, lesions appeared that resembled ductal carcinoma *in situ*, and by five months animals presented with multifocal infiltrating ductal carcinomas (Fig. 1E). Wild-type animals fed the

GW diet exhibited ductal hyperplasia at 11 weeks, but no other histological abnormalities (Fig. 1C, Supplementary Fig. 1E).

Previously we reported that GW increased PPARδ, pPDK1 and pT308Akt expression in the mammary gland of wild-type mice (30). To assess the progressive changes in this signaling pathway, mammary tissue and tumors were analyzed at varying intervals after administration of the GW diet (Fig. 2). Mammary tissue was positive for PPARδ, pT308Akt, pmTor and pS6, as well as the trophoblast protein Plac1, throughout treatment. Tumors were positive for estrogen receptor (ER) and progesterone receptor (PR), and negative for ErbB2, a rare phenotype for genetically engineered breast cancer mouse models (41).

mTor activation and everolimus treatment

Since mTor signaling paralleled tumorigenesis, animals maintained on the GW diet for 6 weeks were treated during the last two weeks on the diet with the mTor inhibitor everolimus/RAD001 administered by daily gavage at doses of 10 and 20 mg/kg (Fig. 3). Everolimus reverted many of the aberrant premalignant changes in the mammary gland as assessed by whole mounts (Fig. 3A) and H&E staining (Fig. 3B), which correlated with inhibition of pS235/236S6 (Fig. 3C,D) and Ki-67 (Fig. 3D), but not with changes in pT308Akt, pS473Akt, pmTor, p4EBP and pAMPKα1 (Fig. 3C). Administration of 20 mg/kg everolimus to mice maintained on the GW diet for four months resulted in similar histological changes towards a less malignant phenotype (results not shown).

Gene microarray analysis of everolimus-treated animals revealed several differences between PPARδ-responsive and everolimus-sensitive gene expression (Fig. 3E, F and Supplementary Table 3). Treatment with 10 mg/kg everolimus resulted in changes in 71 genes, of which 70% contained PPAR response elements (PPREs) (Supplementary Table 3). Everolimus down-regulated expression of PPRE-containing genes associated with differentiation (Krt79, Ltf and Pvalb), inflammation (Saa1/2), invasion (Klk6/7/10 and Cst6), metabolism (Ppp1r3a, Eno3, Cox6a2, Apobec2, Pgam2 and Ckmt2) and motility (18 myosin-, actin- and troponin-related genes), but did not significantly affect several proliferation- (Calm4, Mycl1, Sncg and Plac1), transport- (Npr3) and transcription- (Zbtb16 and Foxi1)-associated genes, including PPARδ. Overall, many, but not all changes in the mammary gland elicited by PPARδ activation are mediated by the mTor signaling pathway.

Differential gene expression by PPARδ activation

To determine the progressive changes induced in gene expression, analyses were carried out with mammary tissue from transgenic and wild-type mice maintained for one or 11 weeks on the GW diet (Table 1). Both groups of animals exhibited a common 10 gene PPRE gene signature vs. similarly treated wild-type mice, which encompassed inflammation, invasion, proliferation and metabolism. The gene expression profile of transgenic mice fed the GW diet for 11 weeks is shown in Fig. 4A, B and Supplementary Table 4. Of the 34 genes up-regulated in GW-treated PPARδ mice, 70% contained PPREs, including genes associated with differentiation (Anxa8 and Krt14), inflammation (Saa1/2/3, S100A8/9, Il1b, Ccl8 and Ptgs2), invasion (Klk6/7/11 and Mmp12), metabolism, (Acsl4 and Crabp1), proliferation (Plac1 and Ccnb1) and transport (Aqp3, Gpr172b and Slc34a2). In contrast, the gene expression signature of 15 week-old age-matched transgenic mice fed a standard diet included >150 genes, of which 50% contained PPREs (Supplementary Table 5). Approximately 40% of the up-regulated genes were associated with mitosis and proliferation, and although consistent with the oncogenic phenotype, were not altered in PPARδ mice treated with GW for 11 weeks. Similarly treated wild-type mice exhibited changes in >130 genes, of which 55% contained PPREs (Supplementary Table 6). Within

this profile, only the PPRE-containing motility-associated genes Ttn, Smpx, Myot, Myh4, Myh2, Trdn and Lbd3 were common to the expression profile in untreated transgenic mice, suggesting that most of the changes in gene expression in GW-treated wild-type mice were ancillary to oncogenesis.

Metabolomic analysis

To delineate the early metabolic consequences of transgene activation, metabolomic analysis was carried out with mammary tissue from wild-type and transgenic mice maintained on the standard or GW-supplemented diets for 11 weeks (Table 2, Fig. 4C, Supplementary Fig. 2). GW-treated PPARδ mice, in comparison to similarly treated wild-type mice, exhibited a marked increase in the levels of phosphatidylcholine (PC) metabolites, arachidonic acid, LPA and PA. These changes were consistent with the changes in PPARδ-regulated genes, including Pla2 and Ptgs2 involved in prostaglandin biosynthesis (Supplementary Table 4), and LPA and PA-mediated activation of mTor (Fig. 4D).

DISCUSSION

The present study describes the first transgenic animal model in which activation of the nuclear receptor PPARδ induces mammary tumorigenesis. Infiltrating adenocarcinomas occurred in all animals within 12 months, and the oncogenic process was rapidly accelerated by activation of the receptor by the agonist GW. In the latter instance, ductal and lobular hyperplasia, dysplasia and DCIS-like lesions occurred in a stochastic manner over several weeks. Although, the potency of the synthetic ligand likely contributed to the shorter latency of tumor formation, it may also have reflected production of endogenous ligands, including prostaglandins, phospholipids and unsaturated fatty acids (26, 27, 29, 47) generated downstream of PPARδ activation as noted previously (30, 47) and in this study (Table 2, Fig. 4C). Although, our studies were carried out with one founder line that exhibited high transgene expression, random transgene insertion and activation of another locus may have contributed to the phenotype. However, we consider this possibility unlikely since tumorigenesis was accelerated by the PPARδ ligand GW, which resulted in similar protein and gene expression profiles in unstimulated and stimulated animals. Off-target effects of GW may also have contributed to the observed phenotype, but this would not appreciably affect the interpretation of our data for two reasons. First, the dose of GW (6) is equivalent to a daily oral dose of 5 mg/kg that was previously shown to specifically enhance PPARδ-dependent metabolism (48), and its congener, GW7042, did not alter gene expression in PPARδ knockout mice (49). Secondly, the gene expression pattern elicited by GW in transgenic mice was unique in comparison to similarly treated wild-type animals.

A signature feature of MMTV-PPARδ mice was the development of $ER^+/PR^+/ErbB2^-$ tumors, characteristics that define the luminal subtype of breast cancer (50). Luminal breast cancer has been further defined by gene expression profiling into subtypes A and B, where type B denotes lower ER expression, higher Ki-67 staining and a higher histologic grade. By these criteria, tumors arising in PPARδ transgenic mice resemble more the luminal B subtype. Since ER mRNA was relatively low in comparison to immunochemical staining, these results also suggest that post-transcriptional regulation of ER may be an important factor in ER expression in PPARδ mice, eg. mTor-mediated ER phosphorylation (51). Additionally, we previously noted increased ER^+ mammary tumors following carcinogenesis in dominant-negative MMTV-Pax8PPARγ transgenic mice (37) and in wild-type FVB mice treated with the irreversible PPARγ inhibitor GW9662 (52), which supports the concept that PPARγ and PPARδ, either by direct competition (53), cofactor competition (54) and/or ligand-dependent activation and repression (55), have opposing actions that ultimately influence the expansion of the ER^+/PR^+ mammary progenitor lineage. Since other MMTV transgenic mouse models, with the exception of MMTV-AIB1 transgenic mice (56,

57), lack the ER^+ luminal phenotype (41), this suggests that the PPARδ transgene, rather than the MMTV promoter, drives expansion of the ER^+ progenitor lineage. This conclusion is further implied by the similarity between MMTV-AIB1 and MMTV-PPARδ mice in activating the Akt/mTor signaling axis (56, 57), suggesting a scenario where ligand-dependent co-activator recruitment to PPARδ leads to ER^+ progenitor cell expansion and oncogenesis.

The progressive histopathological changes resulting from PPARδ activation were associated with up-regulation of Plac1, a microvillous membrane protein expressed primarily in trophoblasts and not in other somatic tissues except for low levels in the testes (58). Plac1 expression occurred in transgenic mice, but not to wild-type mice, as early as one week after administration of GW (Fig. 1, Table 1), and correlated with the early onset of oncogenesis. Plac1 was reported to be re-expressed in several malignancies (59–61), and reduction of Plac1 in breast cancer cells inhibited proliferation and invasion (59). This suggests that Plac1 may serve as an early marker of oncogenesis or possibly a therapeutic target, as suggested by the more favorable prognosis of colorectal cancer patients expressing Plac1 autoantibodies (62). Analysis of a limited set of paired breast cancer specimens indicated that Plac1 was elevated in all tumor specimens (unpublished results), confirming previous results of changes in Plac1 RNA levels (59, 60). Our data suggest that Plac1 transcription is regulated by PPARδ, but not by mTor, although everolimus did reduce protein levels. Many of the transcription factors driving transcription of human Plac1 are associated with C/EBPα and C/EBPβ (63), which is consistent with their role as coactivators in complex with PPARδ (64). Although, the human and mouse *Plac1* promoter regions were reported to be up-regulated by LXR and RXRα (65), neither PPARδ agonists nor co-expression with PPARδ were tested, leaving open the question of the direct involvement of PPARδ in the regulation of *Plac1* transcription.

PPARδ activation was associated with Akt and mTor activation as denoted by enhanced pT308Akt and pS6. These results agree with previous studies showing that pAkt and pS6 (66–68), but not p4EBP (69), were the best surrogate markers of everolimus activity in experimental tumor models and patients. Everolimus resolved many of the early aberrant histopathological changes resulting from PPARδ activation that may have resulted from indirect or direct mTOR activation by LPA and PA, respectively (70, 71) (Table 2, Fig. 4D). This was unexpected in view of positive effect of PPARδ on fatty acid oxidation in skeletal muscle and fat (72, 73). Gene expression and metabolomic profiling however, suggest that PPARδ up-regulates genes essential for promoting a lipogenic phenotype that lead to increased PC, LPA and PA biosynthesis, which presumably drive activation of the mTor axis directly (71) and indirectly through G protein-coupled receptors (74). Since long-term testing of everolimus has not been evaluated thus far, we do not know whether mTor signaling is a major contributor to the malignant changes stemming from PPARδ activation. From a transcriptional standpoint, the *mTor* promoter does not contain PPREs, but the promoter regions of Akt2 and Akt3, but not Akt1, do contain these response elements. Akt can activate mTor directly (75) and indirectly through activation of Tsc and inhibition of Rheb (76). Additionally, the ability of PPARδ to activate Akt is a prerequisite for its growth promoting and anti-apoptotic effects (11, 32, 33), including the wound-healing response (77, 78). Thus, modulation of this pathway by PPARδ appears to be a key event in the tumorigenic phenotype exhibited in this mouse model.

Lastly, the inflammatory factors Saa1, Saa2, S100a8 and S100a9, as well as several members of the kallikrein gene family were selectively increased in GW-treated PPARδ mice (Table 1), and have been reported to be elevated in ER^+ breast cancer (79, 80). S100A8 and S100A9 act as ligands for Ager (advanced glycation end-product receptor) and mediate acute and chronic inflammation, tumor development and metastasis (81, 82), processes

previously associated with GW-dependent gastric carcinogenesis (83) and psoriasis (84). This paradigm is consistent with GW-induced activation of Ptges and Ptgs2/Cox-2 expression (85, 86), which initiate the biosynthesis of arachidonic acid and phospholipid metabolites that can serve as PPARδ ligands (Fig. 4D). Since over-expression of Ptgs2 in the mammary gland is oncogenic (87), one would expect that PPARδ and inflammation would contribute cooperatively to the development of tumorigenesis in this model.

In summary, we describe a novel $ER^{+/}PR^{+}/ErbB2^{-}$ breast cancer model that is dependent on the activation of PPARδ and its ability to elicit an inflammatory, invasive, metabolic and proliferative response that culminates in Akt/mTor activation, which could potentially drive genomic instability (Supplementary Figure 3). This animal model should prove useful for delineating the role of PPARδ in tumor initiation and progression, and as a possible target for early intervention.

Supplementary Material

Refer to Web version on PubMed Central for supplementary material.

Acknowledgments

This work was supported by grant 1R01 CA111482 and contract 1NO1 CN43302-WA19 from the National Cancer Institute, NIH, and award 1P30 CA051008 from the National Cancer Institute, NIH to the Lombardi Comprehensive Cancer Center. This investigation was conducted using the Animal Research, Genomics and Epigenomics and Microscopy and Imaging Shared Resources of the LCCC, and by an animal facilities construction grant from the NIH.

References

1. Berger JP, Akiyama TE, Meinke PT. PPARs: therapeutic targets for metabolic disease. Trends Pharmacol Sci. 2005; 26:244–51. [PubMed: 15860371]
2. Michalik L, Desvergne B, Wahli W. Peroxisome-proliferator-activated receptors and cancers: complex stories. Nature reviews Cancer. 2004; 4:61–70.
3. Hansen JB, Zhang H, Rasmussen TH, Petersen RK, Flindt EN, Kristiansen K. Peroxisome proliferator-activated receptor delta (PPARdelta)-mediated regulation of preadipocyte proliferation and gene expression is dependent on cAMP signaling. J Biol Chem. 2001; 276:3175–82. [PubMed: 11069900]
4. Jehl-Pietri C, Bastie C, Gillot I, Luquet S, Grimaldi PA. Peroxisome-proliferator-activated receptor delta mediates the effects of long-chain fatty acids on post-confluent cell proliferation. Biochem J. 2000; 350(Pt 1):93–8. [PubMed: 10926831]
5. Pelton P. GW-501516 GlaxoSmithKline/Ligand. Curr Opin Investig Drugs. 2006; 7:360–70.
6. Yin Y, Russell RG, Dettin LE, Bai R, Wei ZL, Kozikowski AP, et al. Peroxisome proliferator-activated receptor delta and gamma agonists differentially alter tumor differentiation and progression during mammary carcinogenesis. Cancer Res. 2005; 65:3950–7. [PubMed: 15867396]
7. Glazer RI, Yuan H, Xie Z, Yin Y. PPARgamma and PPARdelta as modulators of neoplasia and cell fate. PPAR research. 2008; 2008:247379. [PubMed: 18566686]
8. Peters JM, Shah YM, Gonzalez FJ. The role of peroxisome proliferator-activated receptors in carcinogenesis and chemoprevention. Nature reviews Cancer. 2012; 12:181–95.
9. Gupta RA, Wang D, Katkuri S, Wang H, Dey SK, DuBois RN. Activation of nuclear hormone receptor peroxisome proliferator-activated receptor-delta accelerates intestinal adenoma growth. Nat Med. 2004
10. Wang D, Wang H, Guo Y, Ning W, Katkuri S, Wahli W, et al. Crosstalk between peroxisome proliferator-activated receptor delta and VEGF stimulates cancer progression. Proc Natl Acad Sci U S A. 2006; 103:19069–74. [PubMed: 17148604]

11. Han S, Ritzenthaler JD, Zheng Y, Roman J. PPARbeta/delta agonist stimulates human lung carcinoma cell growth through inhibition of PTEN expression: the involvement of PI3K and NF-kappaB signals. Am J Physiol Lung Cell Mol Physiol. 2008; 294:L1238–49. [PubMed: 18390835]
12. Stephen RL, Gustafsson MC, Jarvis M, Tatoud R, Marshall BR, Knight D, et al. Activation of peroxisome proliferator-activated receptor delta stimulates the proliferation of human breast and prostate cancer cell lines. Cancer Res. 2004; 64:3162–70. [PubMed: 15126355]
13. Suchanek KM, May FJ, Lee WJ, Holman NA, Roberts-Thomson SJ. Peroxisome proliferator-activated receptor beta expression in human breast epithelial cell lines of tumorigenic and non-tumorigenic origin. Int J Biochem Cell Biol. 2002; 34:1051–8. [PubMed: 12009300]
14. Girroir EE, Hollingshead HE, Billin AN, Willson TM, Robertson GP, Sharma AK, et al. Peroxisome proliferator-activated receptor-beta/delta (PPARbeta/delta) ligands inhibit growth of UACC903 and MCF7 human cancer cell lines. Toxicology. 2008; 243:236–43. [PubMed: 18054822]
15. Park BH, Vogelstein B, Kinzler KW. Genetic disruption of PPARdelta decreases the tumorigenicity of human colon cancer cells. Proc Natl Acad Sci U S A. 2001; 98:2598–603. [PubMed: 11226285]
16. Kwak H, Hwang I, Kim JH, Kim MY, Yang JS, Jeong S. Modulation of transcription by the peroxisome proliferator-activated receptor delta--binding RNA aptamer in colon cancer cells. Molecular cancer therapeutics. 2009; 8:2664–73. [PubMed: 19723884]
17. Ghosh M, Ai Y, Narko K, Wang Z, Peters JM, Hla T. PPARdelta is pro-tumorigenic in a mouse model of COX-2-induced mammary cancer. Prostaglandins Other Lipid Mediat. 2009; 88:97–100. [PubMed: 19101649]
18. Barak Y, Liao D, He W, Ong ES, Nelson MC, Olefsky JM, et al. Effects of peroxisome proliferator-activated receptor delta on placentation, adiposity, and colorectal cancer. Proc Natl Acad Sci U S A. 2002; 99:303–8. [PubMed: 11756685]
19. Zuo X, Peng Z, Moussalli MJ, Morris JS, Broaddus RR, Fischer SM, et al. Targeted genetic disruption of peroxisome proliferator-activated receptor-delta and colonic tumorigenesis. J Natl Cancer Inst. 2009; 101:762–7. [PubMed: 19436036]
20. Abdollahi A, Schwager C, Kleeff J, Esposito I, Domhan S, Peschke P, et al. Transcriptional network governing the angiogenic switch in human pancreatic cancer. Proc Natl Acad Sci U S A. 2007; 104:12890–5. [PubMed: 17652168]
21. Kittler R, Zhou J, Hua S, Ma L, Liu Y, Pendleton E, et al. A Comprehensive Nuclear Receptor Network for Breast Cancer Cells. Cell reports. 2013
22. Hursting SD, Hursting MJ. Growth signals, inflammation, and vascular perturbations: mechanistic links between obesity, metabolic syndrome, and cancer. Arterioscler Thromb Vasc Biol. 2012; 32:1766–70. [PubMed: 22815342]
23. Barish GD, Narkar VA, Evans RM. PPAR delta: a dagger in the heart of the metabolic syndrome. J Clin Invest. 2006; 116:590–7. [PubMed: 16511591]
24. Gupta RA, Tan J, Krause WF, Geraci MW, Willson TM, Dey SK, et al. Prostacyclin-mediated activation of peroxisome proliferator-activated receptor delta in colorectal cancer. Proc Natl Acad Sci U S A. 2000; 97:13275–80. [PubMed: 11087869]
25. Yoshinaga M, Kitamura Y, Chaen T, Yamashita S, Tsuruta S, Hisano T, et al. The simultaneous expression of peroxisome proliferator-activated receptor delta and cyclooxygenase-2 may enhance angiogenesis and tumor venous invasion in tissues of colorectal cancers. Dig Dis Sci. 2009; 54:1108–14. [PubMed: 18720000]
26. Naruhn S, Meissner W, Adhikary T, Kaddatz K, Klein T, Watzer B, et al. 15-hydroxyeicosatetraenoic acid is a preferential peroxisome proliferator-activated receptor beta/delta agonist. Mol Pharmacol. 2010; 77:171–84. [PubMed: 19903832]
27. Forman BM, Chen J, Evans RM. Hypolipidemic drugs, polyunsaturated fatty acids, and eicosanoids are ligands for peroxisome proliferator-activated receptors alpha and delta. Proc Natl Acad Sci U S A. 1997; 94:4312–7. [PubMed: 9113986]
28. Xu HE, Lambert MH, Montana VG, Parks DJ, Blanchard SG, Brown PJ, et al. Molecular recognition of fatty acids by peroxisome proliferator-activated receptors. Mol Cell. 1999; 3:397–403. [PubMed: 10198642]

29. Yu K, Bayona W, Kallen CB, Harding HP, Ravera CP, McMahon G, et al. Differential activation of peroxisome proliferator-activated receptors by eicosanoids. J Biol Chem. 1995; 270:23975–83. [PubMed: 7592593]
30. Pollock CB, Yin Y, Yuan H, Zeng X, King S, Li X, et al. PPARdelta activation acts cooperatively with 3-phosphoinositide-dependent protein kinase-1 to enhance mammary tumorigenesis. PloS one. 2011; 6:e16215. [PubMed: 21297860]
31. Di-Poi N, Michalik L, Tan NS, Desvergne B, Wahli W. The anti-apoptotic role of PPARbeta contributes to efficient skin wound healing. J Steroid Biochem Mol Biol. 2003; 85:257–65. [PubMed: 12943711]
32. Di-Poi N, Tan NS, Michalik L, Wahli W, Desvergne B. Antiapoptotic role of PPARbeta in keratinocytes via transcriptional control of the Akt1 signaling pathway. Mol Cell. 2002; 10:721–33. [PubMed: 12419217]
33. Pedchenko TV, Gonzalez AL, Wang D, DuBois RN, Massion PP. Peroxisome proliferator-activated receptor beta/delta expression and activation in lung cancer. Am J Respir Cell Mol Biol. 2008; 39:689–96. [PubMed: 18566335]
34. Liu P, Cheng H, Roberts TM, Zhao JJ. Targeting the phosphoinositide 3-kinase pathway in cancer. Nature reviews Drug discovery. 2009; 8:627–44.
35. Ackler S, Ahmad S, Tobias C, Johnson MD, Glazer RI. Delayed mammary gland involution in MMTV-AKT1 transgenic mice. Oncogene. 2002; 21:198–206. [PubMed: 11803463]
36. Wei ZL, Kozikowski AP. A short and efficient synthesis of the pharmacological research tool GW501516 for the peroxisome proliferator-activated receptor delta. J Org Chem. 2003; 68:9116–8. [PubMed: 14604391]
37. Yin Y, Yuan H, Zeng X, Kopelovich L, Glazer RI. Inhibition of peroxisome proliferator-activated receptor gamma increases estrogen receptor-dependent tumor specification. Cancer Res. 2009; 69:687–94. [PubMed: 19147585]
38. Amri EZ, Bonino F, Ailhaud G, Abumrad NA, Grimaldi PA. Cloning of a protein that mediates transcriptional effects of fatty acids in preadipocytes. Homology to peroxisome proliferator-activated receptors. J Biol Chem. 1995; 270:2367–71. [PubMed: 7836471]
39. Upadhyay G, Yin Y, Yuan H, Li X, Derynck R, Glazer RI. Stem cell antigen-1 enhances tumorigenicity by disruption of growth differentiation factor-10 (GDF10)-dependent TGF-{beta} signaling. Proc Natl Acad Sci U S A. 2011; 108:7820–5. [PubMed: 21518866]
40. Yin Y, Bai R, Russell RG, Beildeck ME, Xie Z, Kopelovich L, et al. Characterization of medroxyprogesterone and DMBA-induced multilineage mammary tumors by gene expression profiling. Mol Carcinog. 2005; 44:42–50. [PubMed: 15937957]
41. Herschkowitz JI, Simin K, Weigman VJ, Mikaelian I, Usary J, Hu Z, et al. Identification of conserved gene expression features between murine mammary carcinoma models and human breast tumors. Genome biology. 2007; 8:R76. [PubMed: 17493263]
42. Patterson AD, Li H, Eichler GS, Krausz KW, Weinstein JN, Fornace AJ Jr, et al. UPLC-ESI-TOFMS-based metabolomics and gene expression dynamics inspector self-organizing metabolomic maps as tools for understanding the cellular response to ionizing radiation. Anal Chem. 2008; 80:665–74. [PubMed: 18173289]
43. Tautenhahn R, Patti GJ, Rinehart D, Siuzdak G. XCMS Online: a web-based platform to process untargeted metabolomic data. Anal Chem. 2012; 84:5035–9. [PubMed: 22533540]
44. Patti GJ, Tautenhahn R, Siuzdak G. Meta-analysis of untargeted metabolomic data from multiple profiling experiments. Nature protocols. 2012; 7:508–16.
45. Stewart TA, Pattengale PK, Leder P. Spontaneous mammary adenocarcinomas in transgenic mice that carry and express MTV/myc fusion genes. Cell. 1984; 38:627–37. [PubMed: 6488314]
46. Yu J, Leung WK, Chen J, Ebert MP, Malfertheiner P, Sung JJ. Expression of peroxisome proliferator-activated receptor delta in human gastric cancer and its response to specific COX-2 inhibitor. Cancer Lett. 2005; 223:11–7. [PubMed: 15890232]
47. Barroso E, Rodriguez-Calvo R, Serrano-Marco L, Astudillo AM, Balsinde J, Palomer X, et al. The PPARbeta/delta activator GW501516 prevents the down-regulation of AMPK caused by a high-fat diet in liver and amplifies the PGC-1alpha-Lipin 1-PPARalpha pathway leading to increased fatty acid oxidation. Endocrinology. 2011; 152:1848–59. [PubMed: 21363937]

48. Tanaka T, Yamamoto J, Iwasaki S, Asaba H, Hamura H, Ikeda Y, et al. Activation of peroxisome proliferator-activated receptor delta induces fatty acid beta-oxidation in skeletal muscle and attenuates metabolic syndrome. Proc Natl Acad Sci U S A. 2003; 100:15924–9. [PubMed: 14676330]
49. Palkar PS, Borland MG, Naruhn S, Ferry CH, Lee C, Sk UH, et al. Cellular and pharmacological selectivity of the peroxisome proliferator-activated receptor-beta/delta antagonist GSK3787. Mol Pharmacol. 2010; 78:419–30. [PubMed: 20516370]
50. Sotiriou C, Pusztai L. Gene-expression signatures in breast cancer. N Engl J Med. 2009; 360:790–800. [PubMed: 19228622]
51. Yamnik RL, Holz MK. mTOR/S6K1 and MAPK/RSK signaling pathways coordinately regulate estrogen receptor alpha serine 167 phosphorylation. FEBS Lett. 2010; 584:124–8. [PubMed: 19925796]
52. Yuan H, Kopelovich L, Yin Y, Lu J, Glazer RI. Drug-targeted inhibition of peroxisome proliferator-activated receptor-gamma enhances the chemopreventive effect of anti-estrogen therapy. Oncotarget. 2012; 3:345–56. [PubMed: 22538444]
53. Shi Y, Hon M, Evans RM. The peroxisome proliferator-activated receptor delta, an integrator of transcriptional repression and nuclear receptor signaling. Proc Natl Acad Sci U S A. 2002; 99:2613–8. [PubMed: 11867749]
54. Gustafsson MC, Knight D, Palmer CN. Ligand modulated antagonism of PPARgamma by genomic and non-genomic actions of PPARdelta. PloS one. 2009; 4:e7046. [PubMed: 19756148]
55. Adhikary T, Kaddatz K, Finkernagel F, Schonbauer A, Meissner W, Scharfe M, et al. Genomewide analyses define different modes of transcriptional regulation by peroxisome proliferator-activated receptor-beta/delta (PPARbeta/delta). PloS one. 2011; 6:e16344. [PubMed: 21283829]
56. Torres-Arzayus MI, Yuan J, DellaGatta JL, Lane H, Kung AL, Brown M. Targeting the AIB1 oncogene through mammalian target of rapamycin inhibition in the mammary gland. Cancer Res. 2006; 66:11381–8. [PubMed: 17145884]
57. Torres-Arzayus MI, Font de Mora J, Yuan J, Vazquez F, Bronson R, Rue M, et al. High tumor incidence and activation of the PI3K/AKT pathway in transgenic mice define AIB1 as an oncogene. Cancer cell. 2004; 6:263–74. [PubMed: 15380517]
58. Fant M, Farina A, Nagaraja R, Schlessinger D. PLAC1 (Placenta-specific 1): a novel, X-linked gene with roles in reproductive and cancer biology. Prenat Diagn. 2011; 30:497–502. [PubMed: 20509147]
59. Koslowski M, Sahin U, Mitnacht-Kraus R, Seitz G, Huber C, Tureci O. A placenta-specific gene ectopically activated in many human cancers is essentially involved in malignant cell processes. Cancer Res. 2007; 67:9528–34. [PubMed: 17909063]
60. Silva WA Jr, Gnjatic S, Ritter E, Chua R, Cohen T, Hsu M, et al. PLAC1, a trophoblast-specific cell surface protein, is expressed in a range of human tumors and elicits spontaneous antibody responses. Cancer Immun. 2007; 7:18. [PubMed: 17983203]
61. Dong XY, Peng JR, Ye YJ, Chen HS, Zhang LJ, Pang XW, et al. Plac1 is a tumor-specific antigen capable of eliciting spontaneous antibody responses in human cancer patients. Int J Cancer. 2008; 122:2038–43. [PubMed: 18183594]
62. Liu FF, Dong XY, Pang XW, Xing Q, Wang HC, Zhang HG, et al. The specific immune response to tumor antigen CP1 and its correlation with improved survival in colon cancer patients. Gastroenterology. 2008; 134:998–1006. [PubMed: 18395081]
63. Koslowski M, Tureci O, Biesterfeld S, Seitz G, Huber C, Sahin U. Selective activation of trophoblast-specific PLAC1 in breast cancer by CCAAT/enhancer-binding protein beta (C/EBPbeta) isoform 2. J Biol Chem. 2009; 284:28607–15. [PubMed: 19652226]
64. Brunelli L, Cieslik KA, Alcorn JL, Vatta M, Baldini A. Peroxisome proliferator-activated receptor-delta upregulates 14-3-3 epsilon in human endothelial cells via CCAAT/enhancer binding protein-beta. Circ Res. 2007; 100:e59–71. [PubMed: 17303761]
65. Chen Y, Moradin A, Schlessinger D, Nagaraja R. RXRalpha and LXR activate two promoters in placenta- and tumor-specific expression of PLAC1. Placenta. 2011; 32:877–84. [PubMed: 21937108]

66. O'Reilly T, McSheehy PM. Biomarker Development for the Clinical Activity of the mTOR Inhibitor Everolimus (RAD001): Processes, Limitations, and Further Proposals. Translational oncology. 2010; 3:65–79. [PubMed: 20360931]

67. Mazzoletti M, Bortolin F, Brunelli L, Pastorelli R, Di Giandomenico S, Erba E, et al. Combination of PI3K/mTOR inhibitors: antitumor activity and molecular correlates. Cancer Res. 2011; 71:4573–84. [PubMed: 21602434]

68. Noh WC, Kim YH, Kim MS, Koh JS, Kim HA, Moon NM, et al. Activation of the mTOR signaling pathway in breast cancer and its correlation with the clinicopathologic variables. Breast Cancer Res Treat. 2008; 110:477–83. [PubMed: 17805960]

69. Choo AY, Yoon SO, Kim SG, Roux PP, Blenis J. Rapamycin differentially inhibits S6Ks and 4E-BP1 to mediate cell-type-specific repression of mRNA translation. Proc Natl Acad Sci U S A. 2008; 105:17414–9. [PubMed: 18955708]

70. Lu Y, Yu Q, Liu JH, Zhang J, Wang H, Koul D, et al. Src family protein-tyrosine kinases alter the function of PTEN to regulate phosphatidylinositol 3-kinase/AKT cascades. J Biol Chem. 2003; 278:40057–66. [PubMed: 12869565]

71. Foster DA. Phosphatidic acid signaling to mTOR: signals for the survival of human cancer cells. Biochim Biophys Acta. 2009; 1791:949–55. [PubMed: 19264150]

72. Dressel U, Allen TL, Pippal JB, Rohde PR, Lau P, Muscat GE. The peroxisome proliferator-activated receptor beta/delta agonist, GW501516, regulates the expression of genes involved in lipid catabolism and energy uncoupling in skeletal muscle cells. Mol Endocrinol. 2003; 17:2477–93. [PubMed: 14525954]

73. Roberts LD, Murray AJ, Menassa D, Ashmore T, Nicholls AW, Griffin JL. The contrasting roles of PPARdelta and PPARgamma in regulating the metabolic switch between oxidation and storage of fats in white adipose tissue. Genome biology. 2011; 12:R75. [PubMed: 21843327]

74. Mills GB, Moolenaar WH. The emerging role of lysophosphatidic acid in cancer. Nature reviews Cancer. 2003; 3:582–91.

75. Sekulic A, Hudson CC, Homme JL, Yin P, Otterness DM, Karnitz LM, et al. A direct linkage between the phosphoinositide 3-kinase-AKT signaling pathway and the mammalian target of rapamycin in mitogen-stimulated and transformed cells. Cancer Res. 2000; 60:3504–13. [PubMed: 10910062]

76. Wullschleger S, Loewith R, Hall MN. TOR signaling in growth and metabolism. Cell. 2006; 124:471–84. [PubMed: 16469695]

77. Michalik L, Desvergne B, Tan NS, Basu-Modak S, Escher P, Rieusset J, et al. Impaired skin wound healing in peroxisome proliferator-activated receptor (PPAR)alpha and PPARbeta mutant mice. J Cell Biol. 2001; 154:799–814. [PubMed: 11514592]

78. Tan NS, Michalik L, Noy N, Yasmin R, Pacot C, Heim M, et al. Critical roles of PPAR beta/delta in keratinocyte response to inflammation. Genes Dev. 2001; 15:3263–77. [PubMed: 11751632]

79. Eswaran J, Cyanam D, Mudvari P, Reddy SD, Pakala SB, Nair SS, et al. Transcriptomic landscape of breast cancers through mRNA sequencing. Scientific reports. 2012; 2:264. [PubMed: 22355776]

80. Pierce BL, Ballard-Barbash R, Bernstein L, Baumgartner RN, Neuhouser ML, Wener MH, et al. Elevated biomarkers of inflammation are associated with reduced survival among breast cancer patients. J Clin Oncol. 2009; 27:3437–44. [PubMed: 19470939]

81. Gebhardt C, Nemeth J, Angel P, Hess J. S100A8 and S100A9 in inflammation and cancer. Biochem Pharmacol. 2006; 72:1622–31. [PubMed: 16846592]

82. Ghavami S, Chitayat S, Hashemi M, Eshraghi M, Chazin WJ, Halayko AJ, et al. S100A8/A9: a Janus-faced molecule in cancer therapy and tumorgenesis. Eur J Pharmacol. 2009; 625:73–83. [PubMed: 19835859]

83. Pollock CB, Rodriguez O, Martin PL, Albanese C, Li X, Kopelovich L, et al. Induction of metastatic gastric cancer by peroxisome proliferator-activated receptordelta activation. PPAR research. 2010; 2010:571783. [PubMed: 21318167]

84. Romanowska M, Reilly L, Palmer CN, Gustafsson MC, Foerster J. Activation of PPARbeta/delta causes a psoriasis-like skin disease in vivo. PloS one. 2011; 5:e9701. [PubMed: 20300524]

85. Glinghammar B, Skogsberg J, Hamsten A, Ehrenborg E. PPARdelta activation induces COX-2 gene expression and cell proliferation in human hepatocellular carcinoma cells. Biochem Biophys Res Commun. 2003; 308:361–8. [PubMed: 12901877]

86. Han S, Ritzenthaler JD, Wingerd B, Roman J. Activation of peroxisome proliferator-activated receptor beta/delta (PPARbeta/delta) increases the expression of prostaglandin E2 receptor subtype EP4. The roles of phosphatidylinositol 3-kinase and CCAAT/enhancer-binding protein beta. J Biol Chem. 2005; 280:33240–9. [PubMed: 16061473]

87. Liu CH, Chang SH, Narko K, Trifan OC, Wu MT, Smith E, et al. Overexpression of cyclooxygenase-2 is sufficient to induce tumorigenesis in transgenic mice. J Biol Chem. 2001; 276:18563–9. [PubMed: 11278747]

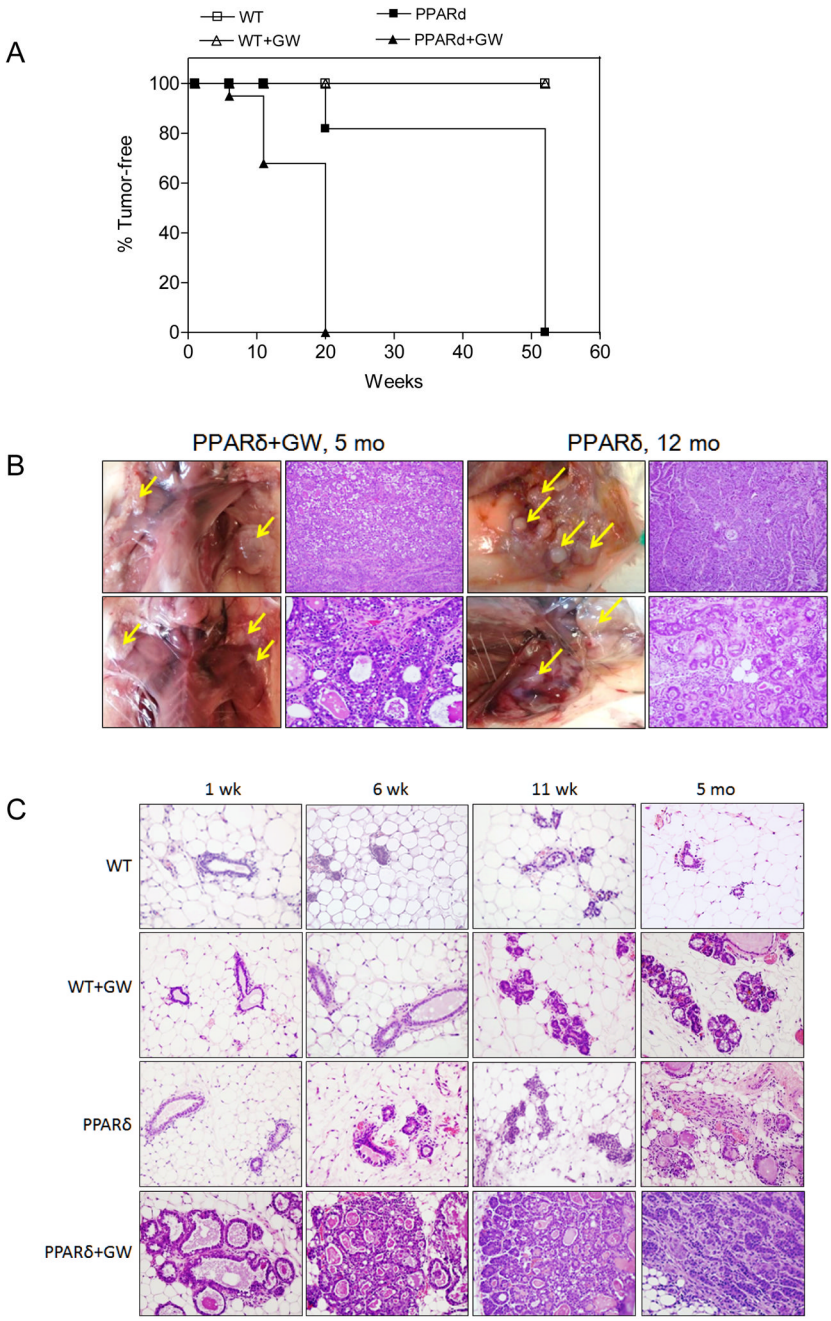

Figure 1. PPARδ activation promotes mammary neoplasia

A, Tumor-free incidence in MMTV-PPARδ mice fed a standard or GW-supplemented diet. Tumor formation differed significantly between untreated or GW501516-treated PPARδ mice (PPARd+GW) vs. untreated or GW-treated wild-type mice (WT+GW) (P<0.0001 by the Chi^2 test). GW-treated PPARδ mice (PPARd+GW) developed tumors more rapidly vs. untreated PPARδ mice (P<0.0001 by the Chi^2 test). Each time point represents tumor incidence as determined by histological examination post-mortem. The number (N) of mice per group at *each* time point was: WT (N=8), WT+GW (N=8), PPARd (N=6), PPARd+GW (N=7). **B**, Tumor formation *in situ*. PPARδ mice fed a standard or GW-supplemented diet presented with multifocal moderate to well-differentiated infiltrating ductal carcinomas at 12

months or five months, respectively. Shown are representative mice from each group. H&E, magnification, 400X. **C**, H&E stained tissue. GW-treated wild-type (WT) exhibited ductal dilitation and secretory changes after six weeks, and increased ductal branching after 11 weeks to five months. PPARδ mice presented with increased ductal branching after six weeks, lobular dysplasia after 11 weeks and areas of neoplasia after five months. GW-treated PPARδ mice exhibited ductal dilatation with lipid droplets and proteinaceous secretions after one week, atypical lobular and ductal hyperplasia after six weeks, atypical ductal dysplasia bordering on ductal carcinoma *in situ* after 11 weeks and infiltrating ductal carcinomas after 5 months. Magnification, 400X.

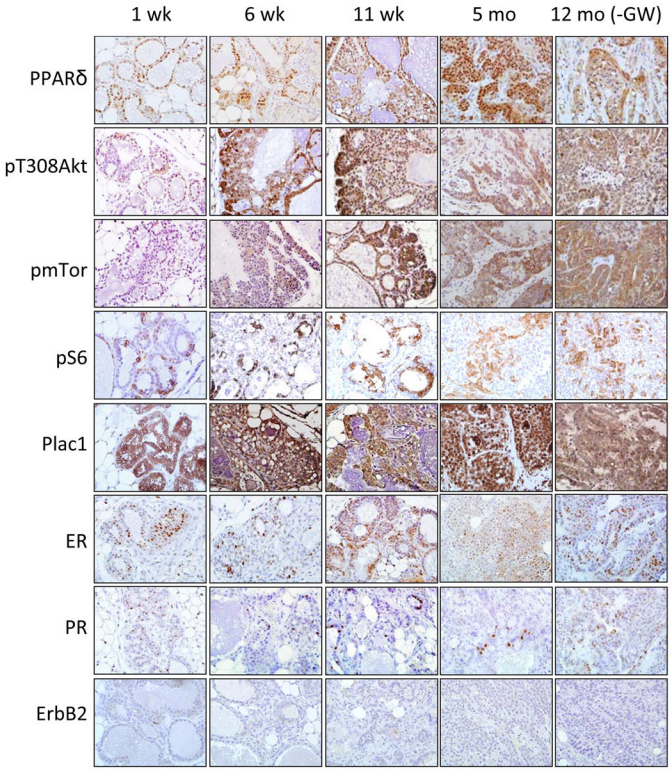

Figure 2. IHC analysis

Sections from mammary tissue were obtained from PPARδ transgenic mice maintained on the GW diet for 1, 6 and 11 weeks and 5 months or for 12 months on a standard diet. Tissue was analyzed for PPARδ, pT308Akt, pmTor, pS6, Plac1, ER, PR and ErbB2 expression. Magnification, 600X.

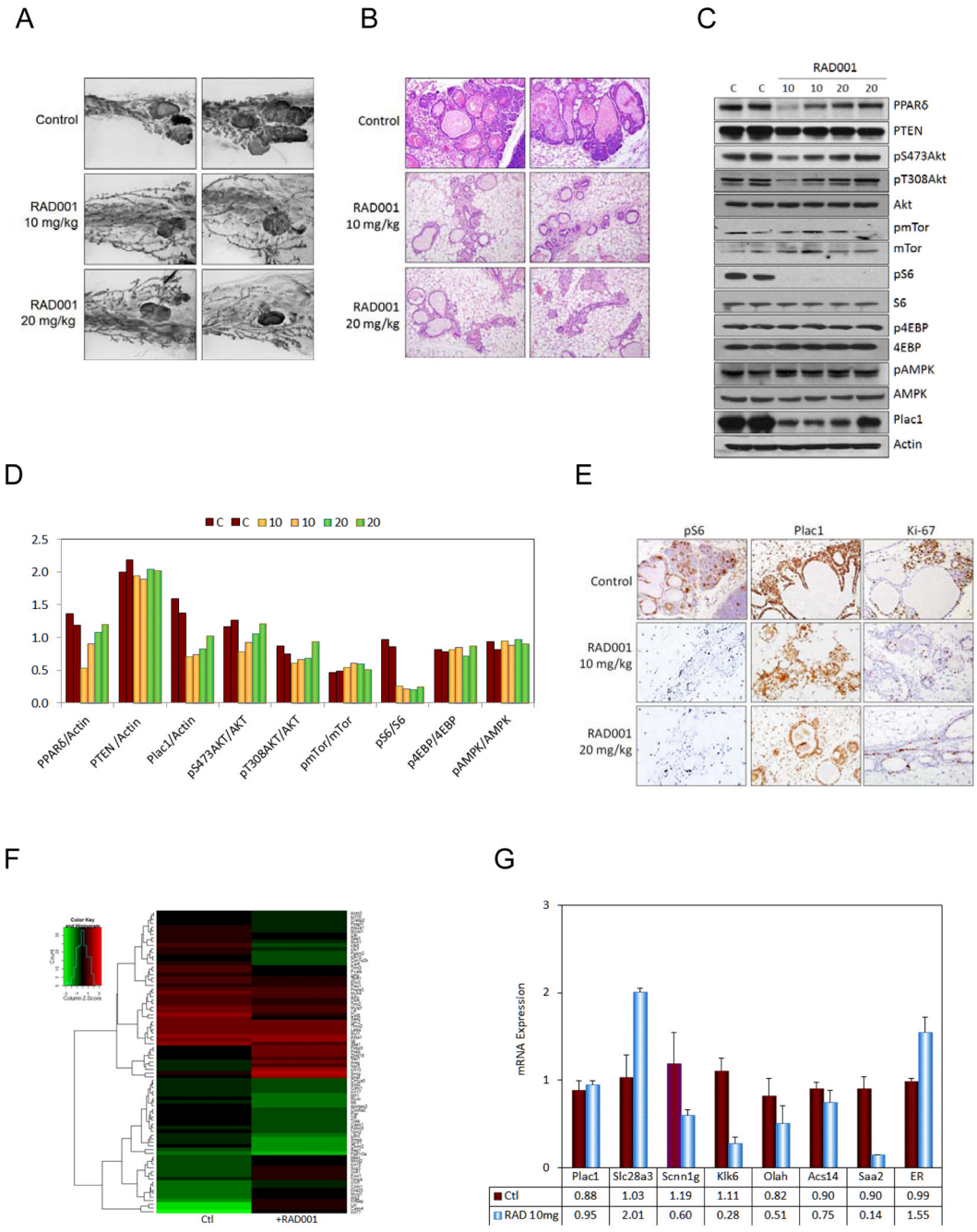

Figure 3. Everolimus suppresses PPARδ and GW501516-mediated changes in the mammary gland and mTor activation

A, Whole mounts. Transgenic mice were maintained on the GW diet for 6 weeks, and treated with 10 mg/kg or 20 mg/kg everolimus daily by gavage during the 5th and 6th weeks on the diet. Everolimus reduced lobular hyperplasia and dysplasia induced by GW in transgenic mice. Magnification, 10X. **B**, H&E stained tissue. Everolimus reduced lobular hyperplasia and dysplasia. Magnification, 400X. **C**, Western blot. Everolimus inhibited S6 phosphorylation (pS6), but did not affect the expression of other signaling molecules. **D**, Quantitation of the western blot in **C. E**, IHC analysis. Everolimus reduced S6 phosphorylation (pS6) and Ki-67 labeling, and had a moderate effect on affect Plac1

expression. Magnification, 400X. **F**, Heat map of genes differentially expressed in PPARδ mice maintained on the GW diet for 6 weeks, and treated with 10 mg/kg everolimus by gavage daily during the 5^{th} and 6^{th} weeks on the diet (see Supplementary Table 3). **G**, qRT-PCR analysis of representative genes in **F**.

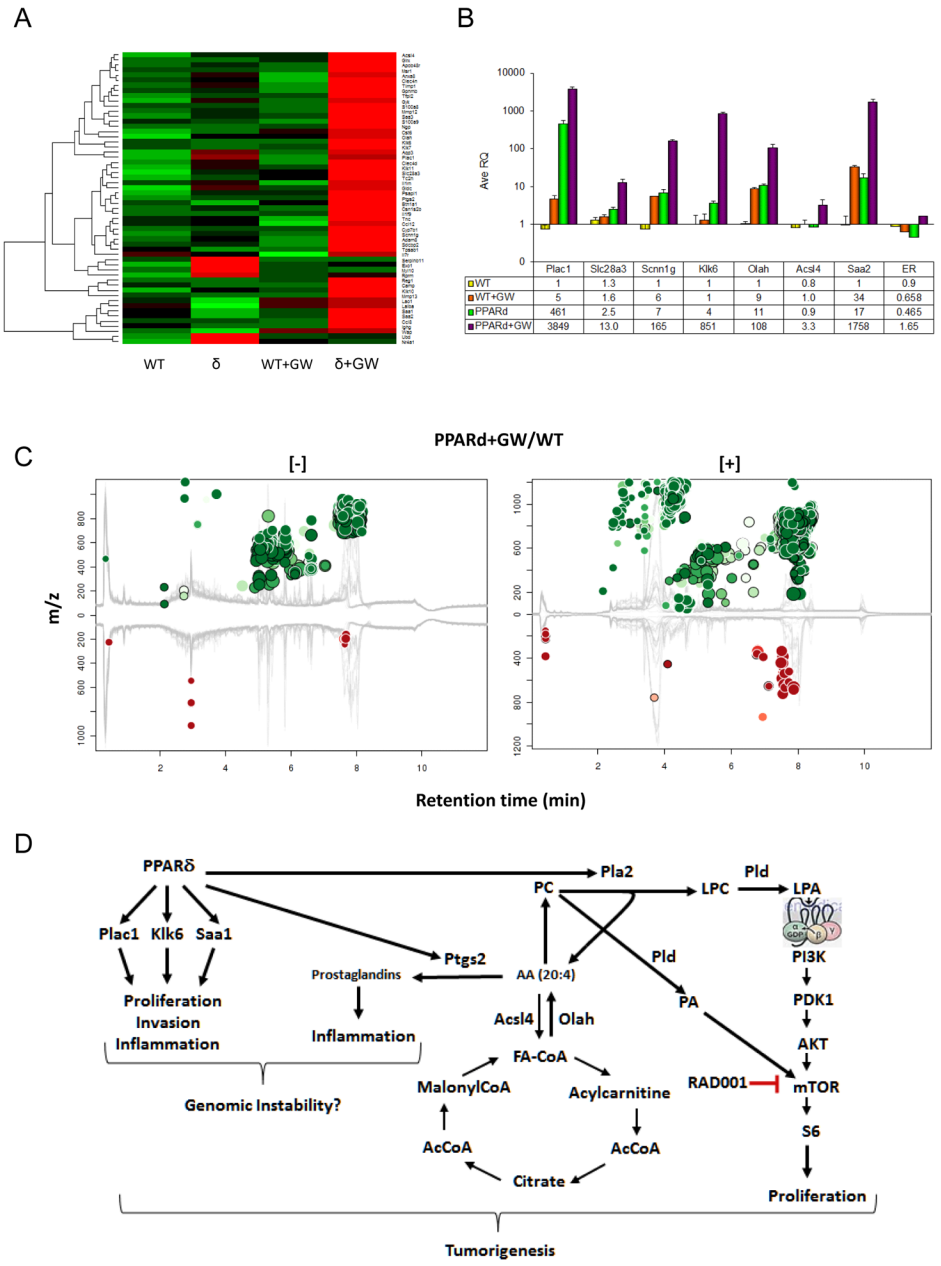

Figure 4. Gene microarray and metabolomic analyses of GW-treated PPARδ mice

A, Shown is a heat map of 34 genes whose expression in mammary tissue was changed >3-fold in PPARδ mice treated with GW for 11 weeks (PPARd+GW) vs. similarly treated wild-type mice (WT+GW) (see Supplementary Table 4). **B**, qRT-PCR analysis of representative genes presented in **A. C**, Mirror plot of metabolites altered in MMTV-PPARδ mice treated as in **A**. Depicted are [+] and [-] Ions whose intensities between groups were altered >5-fold with a p-value <0.01. Ions that were up-regulated are represented as green circles above the plot, and those that were down-regulated are represented as red circles below the plot. The size of each circle corresponds to the log-fold change of the ion, and the shade of the circle represents the p-value, with brighter circles having a lower p-value. The retention time corrected total ion chromatograms are overlaid in gray in the background of the figure. Circles representing features with hits in the METLIN database are shown with a black

outline. **D**, Schematic of alterations in gene expression, metabolism and mTor signaling in MMTV-PPARδ mice treated with GW for 11 weeks. We postulate that activation of PPARδ leads to activation of PPRE-containing genes associated with metabolism (Olah, Ptgs2, Pla2, Pld), proliferation Plac1), invasion (Klk6) and inflammation (Saa1). Increased arachidonic acid (AA) synthesis generated by phospholipse A2 (Pla2) leads to generation of inflammatory prostaglandins Phosphatidylcholine (PC) generates lysophosphatidylcholine (LPC) and lysophosphatidic acid (LPA) through the actions of Pla2) and phospholipase D (Pld). LPA stimulates G protein-coupled receptor activation of mTor through Akt, whereas, PA directly activates mTor. Presumably the net result of these processes contributes to genomic instability.

Table 1

PPARδ-dependent gene expression preferentially altered in GW501516-treated MMTV-PPARδ transgenic mice

Mice at 4 weeks of age were fed a diet containing 0.005% GW501516 for either one or 11 weeks. Shown are ≥3-fold changes in expression in mammary tissue of common PPRE-containing genes with a raw score ≥300 in GW501516 treated MMTV-PPARδ (δ+GW) vs. wild-type littermates treated with GW501516 (WT+GW).

Function Gene Symbol	Raw Score				Ratio
	WT	WT+GW	d	d+GW	d+GW/WT+GW
GW501516 diet for one week:					
Inflammation					
Interleukin 1 family, member 9, Il1f9	18	36	27	356	9.9
S100 calcium binding protein A8 (calgranulin A), S100a8	303	95	238	418	4.4
serum amyloid A1, Saa1	15	90	177	3714	41.3
serum amyloid A2, Saa2	6	47	102	2401	51.1
Invasion/Proliferation					
kallikrein related peptidase 6, Klk6	72	112	61	1255	11.2
kallikrein related peptidase 11, Klk11	23	42	53	823	19.6
placental-specific 1, Plac1	133	132	136	18939	143.2
Metabolism					
acyl-CoA synthetase long-chain family member 4, Acsl4	195	191	183	777	4.1
oleoyl-ACP-hydrolase, Olah	4	6	4	1717	286.2
Transport					
aquaporin 3, Aqp3	37	29	105	5688	194.1
GW501516 diet for 11 weeks:					
Inflammation					
Interleukin 1 family, member 9, Il1f9	58	61	56	629	10.3
S100 calcium binding protein A8 (calgranulin A), S100a8	431	342	415	4266	12.5
serum amyloid A1, Saa1	2715	1742	730	14810	8.5
serum amyloid A2, Saa2	1626	980	409	12963	13.2
Invasion/Proliferation					
kallikrein related-peptidase 6, Klk6	142	106	101	18338	173.1
kallikrein related-peptidase 1, Klk11	36	70	164	722	10.3
placental specific protein 1, Plac1	31	41	1497	4491	108.9

Function Gene Symbol	Raw Score				Ratio
	WT	WT+GW	d	d+GW	d+GW/WT+GW
Metabolism					
acyl-CoA synthetase long-chain family member 4, Acsl4	230	366	372	1287	3.5
oleoyl-ACP-hydrolase, Olah	21	227	237	1361	6.0
Transport					
aquaporin 3, Aqp3	52	114	1230	4438	38.9

Table 2

Metabolites increased in mammary tissue from MMTV-PPARδ mice fed a GW501516 diet

Shown are up-regulated metabolites altered in PPARδ mice fed the GW501516 diet for 11 weeks vs. similarly treated wild-type mice (WT+GW). The features included in the table are based on the XCMS algorithms at: http://xcmsonline.scripps.edu (43).

										Mean Signal Intensity	
molid	**rtmed**	**fold**	**p-value**	**qvalue**	**adduct**	**mass**	**dppm**	**name**	**link**	**WT+GW**	**δ+GW**
39543	8.02	612	1.062E-0	4.306E-04	[M+H]+	809.59	0	PC(18:0/20:4)	Metlin	1253	766334
75868	7.94	583	2.312E-04	5.722E-04	[M+H]+	783.58	0	PC(18:0/18:3)	Metlin	1592	928261
39290	8.05	452	2.700E-05	2.436E-04	[M+H]+	767.55	3	PC(15:0/20:4)	Metlin	191	86277
59955	7.64	410	3.909E-04	7.083E-04	[M+H]+	827.55	2	PC(20:5/20:4)	Metlin	63	25685
59791	8.00	370	4.962E-04	7.861E-04	[M+H]+	833.59	0	PC(20:2/20:4)	Metlin	242	89458
59955	7.75	292	2.597E-04	5.980E-04	[M+H]+	827.55	2	PC(20:5/20:4)	Metlin	69	20120
75636	7.87	148	2.520E-04	5.875E-04	[M+H]+	739.52	2	PC(13:0/20:4)	Metlin	348	51380
59626	7.84	119	4.810E-05	3.117E-04	[M+H]+	803.55	0	PC(18:3/20:4)	Metlin	293	34957
39788	7.88	80	2.740E-04	6.116E-04	[M+H]+	829.56	0	PC(20:4/20:4)	Metlin	140	11131
39248	7.86	69	6.750E-05	3.607E-04	[M+H]+	753.53	0	PC(14:0/20:4)	Metlin	102	7029
59824	8.02	45	4.770E-06	1.174E-04	[M+H]+	831.58	2	PC(20:3/20:4)	Metlin	236	10678
75636	7.57	42	2.517E-04	5.875E-04	[M+H]+	739.52	9	PC(13:0/20:4)	Metlin	69	2907
39290	7.89	33	3.386E-04	6.702E-04	[M+H]+	767.55	6	PC(15:0/20:4)	Metlin	399	13341
81689	7.87	23	2.299E-04	5.71E-04	[M+H]+	786.61	11	PA(20:0/22:1)	Metlin	1137	25751
60185	7.78	17	1.002E-04	4.155E-04	[M+H]+	853.56	0	PC(22:6/20:4)	Metlin	221	3760
75734	7.89	767	8.918E-04	9.084E-04	[M−H]−	765.53	1	PC(15:1/20:4)	Metlin	38	29510
39290	8.03	636	5.670E-05	1.732E-04	[M−H]−	767.55	1	PC(15:0/20:4)	Metlin	34	21790
75636	7.87	416	9.867E-04	9.837E-04	[M−H]−	739.52	1	PC(13:0/20:4)	Metlin	49	20460
39290	7.84	411	8.351E-04	8.885E-04	[M−H]−	767.55	0	PC(15:0/20:4)	Metlin	18	7207
39116	8.07	329	6.060E-05	1.756E-04	[M−H]−	795.58	1	PC(17:0/20:4)	Metlin	8	2512
75853	7.78	277	1.608E-03	1.314E-03	[M−H]−	791.55	3	PC(17:2/20:4)	Metlin	18	5064
40903	7.95	275	5.313E-04	6.584E-04	[M−H]−	741.53	0	PA(18:0/20:4)	Metlin	33	9118
75853	7.99	273	2.113E-04	3.802E-04	[M−H]−	791.55	3	PC(17:2/20:4)	Metlin	30	8204
3406	5.44	244	2.132E-03	1.594E-03	[M−H]−	282.26	1	Oleic acid	Metlin	19	4762
35056	5.02	240	1.032E-03	1.002E-03	[M−H]−	304.24	1	Arachidonic acid	Metlin	37	8881
187	5.33	99	2.263E-03	1.657E-03	[M−H]−	256.24	1	Palmitic acid	Metlin	30	3000

									Mean Signal Intensity		
molid	rtmed	fold	p-value	qvalue	adduct	mass	dppm	name	link	WT+GW	δ+GW
82027	7.84	78	1.262E-03	1.100E-03	[M−H]−	752.54	11	PA(20:0/20:4)	Metlin	18	1408
82006	8.14	58	1.016E-04	2.330E-04	[M−H]−	790.55	7	PA(22:6/21:0)	Metlin	35	2003
40943	5.81	32	1.648E-03	1.328E-03	[M−H]−	438.27	6	LPA(18:0/0:0)	Metlin	23	742